

Disclaimer:

The contents of this report reflect the views of the authors, who are responsible for the facts and the accuracy of the information presented herein. This document is disseminated in the interest of information exchange. The report is funded, partially or entirely, under 69A3552348333 from the U.S. Department of Transportation's University Transportation Centers Program. The U.S. Government assumes no liability for the contents or use thereof.



**Transportation Infrastructure Precast Innovation Center
(TRANS-IPIC)**

University Transportation Center (UTC)

***Thermally Conductive Pre-cast Concrete Pavement for Urban Heat Island
Mitigation***

UT-23-RP-01

**FINAL REPORT
[November 30th, 2024]**

Submitted by:

Islam Radwan, Graduate Student, Islam.Radwan@my.utsa.edu
Samer Dessouky, Professor, Samer.dessouky@utsa.edu
School of Civil & Environmental Engineering and Construction Management
University of Texas at San Antonio

Collaborators / Partners:

Microtek laboratories Company
City of San Antonio
Tindall Corporation

Submitted to:

TRANS-IPIC UTC
University of Illinois Urbana-Champaign
Urbana, IL

Executive Summary:

The urban heat island (UHI) effect poses a significant challenge in urban environments, contributing to increased energy consumption, elevated carbon emissions, deteriorating air quality, and adverse public health outcomes. This study investigates the use of organic microencapsulated phase change materials (PCMs) in precast concrete pavement (sidewalks) as a potential solution to mitigate the UHI effect. Two methods were employed: the Addition Method referred to the percentage of PCM added with respect to total weight of control concrete mix and the Sand Replacement Method referred to percentage of added PCM replacing only the sand in the concrete mix, both at dosage proportions of 0%, 5%, and 10%. The experimental setup was divided into indoor and outdoor environments to assess PCM-enhanced concrete under controlled and real-world conditions. The indoor experiments were further divided into heating and cooling cycles for two phases: 4-hour and 8-hour cycles. The outdoor experiments consisted of a continuous 8-hour cycle, starting from the heat peak at 1 to 9 pm.

Additionally, thermal and material properties such as the thermal heat capacity were measured using a Netzsch 404F1 Pegasus Differential Scanning Calorimeter (DSC), thermal diffusivity was measured using a Netzsch 467HT Laser Flash Analysis (LFA) instrument, and the densities were measured using an Anton Paar Ultrapyc 3000 helium pycnometer. These measurements were crucial for understanding the thermal and material properties of the PCM-integrated concrete and the impact of the PCM on the thermal properties of the concrete.

The results demonstrated significant temperature reductions in PCM-enhanced concrete. In the 4-hour indoor cycles, the addition method reduced surface temperatures by 2°C for 5% PCM and by nearly 8°C for 10% PCM, while the sand replacement method showed reductions of 2°C and 3°C for the 5% and 10% R-PCM samples, respectively. During the 8-hour cycles, the addition method exhibited almost no temperature reduction for the 5% samples, but a 4°C reduction for the 10% PCM sample. Similarly, the sand replacement method showed minimal reduction for the 0% and 5% samples, with a 2°C reduction for the 10% R-PCM sample.

In the outdoor experiments, the addition method showed that the 5% PCM samples had almost a reduction of 2°C, and the 10% PCM sample achieved a significant 7°C reduction over the 8-hour period. The sand replacement method resulted in minimal reduction for the 5% samples about 1.5°C, while the 10% PCM sample showed a reduction of 4°C.

Furthermore, the results indicated higher heat capacity and lower thermal conductivity and diffusivity in the PCM-integrated concrete, with these differences becoming more pronounced as heating progressed. These findings suggest that PCM-enhanced concrete has the potential to mitigate UHI effects by significantly lowering surface temperatures.

This research provides insights into the efficacy of microencapsulated organic PCM in precast concrete rigid pavement (Sidewalks) for UHI mitigation, highlighting the thermal dynamics involved in such applications.

Table of Contents

Statement of Problem	4
Summary of Project Activities	4
Literature Review.....	4
Experimental Design & Material Selection	4
Laboratory Testing	5
Indoor Results -Pavement surface temperature observations by Addition Method	7
Indoor Results -Pavement surface temperature observations by Sand-Replacement Method	8
Materials testing Results	8
Pavement System Design.....	11
Field Implementation and Monitoring	11
Outdoor Results.....	11
Educational outreach and workforce development	12
Technology Transfer	13
Papers that include TRANS-IPIC UTC in the acknowledgments section	13
Number of presentations	13
References	14

Statement of Problem

The Urban Heat Island (UHI) effect refers to higher temperatures in urban areas compared to the surrounding countryside due to human development. Increased thermal energy storage in paving materials contributes to the UHI effect, leading to elevated surface temperatures. Precast concrete pavement with improved mix designs is recognized globally as an emerging technology for mitigating climate change and addressing UHI. These precast elements can be incorporated into innovative pavement systems to enhance mitigation practices, employ efficient construction methods, and promote sustainable pavement restoration. The study investigates the use of precast concrete pavement to create cooler rigid pavement using various cooling mechanisms. These mechanisms involve modifying the thermal properties of pavement materials and reducing heat energy absorption or emission by pavements, while prioritizing environmental sustainability.

Summary of Project Activities

Literature Review

The literature review focuses on three main areas: UHI effects and mitigation strategies, cool pavement techniques, and integration of phase change materials (PCMs) in pavement systems. The UHI effect, characterized by elevated urban temperatures compared to rural areas, arises from the built environment's thermal properties, and reduced evaporative cooling due to impervious surfaces [1-8]. Urban pavements, covering 20–40% of city surfaces, significantly contribute to UHI due to their heat absorption and sensible heat release [9-10]. Cool pavements mitigate UHI by enhancing solar reflectance, promoting evaporation, or using absorbed heat for renewable purposes [11-16]. The PCMs known for their ability to store and release thermal energy during phase transitions, improve the thermal, mechanical, and durability properties of construction materials like concrete [16-17]. PCMs regulate temperature, reduce thermal gradients, and enhance concrete's performance in freezing-thawing cycles, snow melting, and thermal stress management [18-20]. PCM integration methods, such as lightweight aggregate impregnation or embedding PCM in pipes, enhance pavement thermal regulation and snow melting capacity but require careful design to prevent leakage and thermal losses [21-26].

Experimental Design & Material Selection

The experimental design focuses on selecting the appropriate PCM based on its melting point and heat of fusion, as provided by Microtek Laboratories. The selected PCM, in powder form, ensures easy integration with the precast concrete mix as shown in **Figure 1**. Adhering to local standards in San Antonio, Texas, the concrete design mix was formulated considering aggregate gradation and water-cement ratios that meet local TxDOT standards. The mixing process and the dimensions of concrete samples with varying PCM dosages were established as shown in **Figure 2**. Additionally, a heat simulation chamber was designed to observe PCM's behavior in pavement samples. The necessary equipment, including data acquisition system and light bulbs for heating, was acquired to facilitate the experiments as shown in **Figure 3**.



Figure 1: PCM packages.



Figure 2: Concrete - PCM samples with 0%, 5% and 10% by addition and by Sand-Replacement.



Figure 3: Reflective Thermal – Insulated Box Preparation

Laboratory Testing

The experimental work is divided into indoor and outdoor environments. Indoor experiments include first marking and placing the thermocouple sensors on top and bottom surfaces of the concrete samples as shown in **Figure 4**. Both material-based and pavement-based tests were conducted as shown in **Figures 5-7**. Key thermal and material properties were measured using advanced devices. Differential Scanning Calorimetry (DSC) was employed to analyze the heat flow associated with PCM transitions, while Laser Flash Analysis measured thermal diffusivity and conductivity. Additionally, a pycnometer was used to determine the density and porosity of the samples as shown in **Figure 6**. These tests provided critical data on the effectiveness of PCM integration in reducing surface temperatures and enhancing thermal performance of pavement materials. The pavement-based indoor experiments assess how PCM affects surface temperature under controlled conditions for four- and eight-hour cycles heating and cooling. The outdoor experiments are entirely pavement-based, where all samples are exposed to natural sunlight and environmental conditions during the peak heat of the day, from 1 to 9 pm, for a total of 8 hours. These outdoor tests are crucial for understanding the field performance of PCM-enhanced concrete in mitigating temperature variations in pavements.



Figure 4: Marking and Installing Thermocouple Sensors on Top and Bottom Surfaces.



Figure 5: Indoor Heating Experiment set-up; Heating phase; Cooling phase.



Differential Scanning Calorimeter (DSC)

Laser Flash Analysis (LFA)

Gas Pycnometer

Figure 6: Thermal Properties Testing Devices

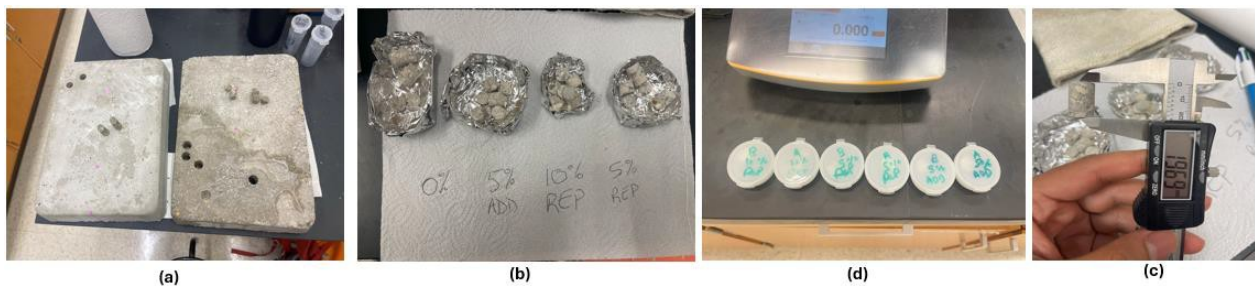


Figure 7: Sample Preparation for the LFA, (a) Coring the slabs, (b) Dried Samples. (c) measuring diameters and thicknesses, (d) final desired samples.

Indoor Results -Pavement surface temperature observations by Addition Method

The surface temperature profiles during the heating and cooling cycles for concrete samples with 0%, 5%, and 10% PCM are shown in **Figure 8**, respectively. For the 0% PCM sample as in **Figure 8a**, the temperature on the top surface rises more quickly and reaches a higher peak compared to the bottom surface in **Figure 8b** during the heating cycle. During the cooling cycle in **Figure 8c**, the temperature decreases steadily, with the top surface cooling faster than the bottom surface as shown in **Figure 8d**. In contrast, the 5% PCM sample as in **Figure 8a** shows a noticeable reduction in temperature rise during the heating cycle. The top surface still heats up faster than the bottom, but the peak temperatures are approximately 2°C lower than those of the 0% PCM sample in **Figure 8a**. The cooling cycle also demonstrates a slower temperature decrease, indicating the PCM's ability to retain heat in **Figures 8c and 8d**. The 10% PCM sample as in **Figure 8a** exhibits the most significant impact of PCM. The temperature rise during the heating cycle is substantially lower for both surfaces, with a peak temperature reduction of about 8°C compared to the 0% PCM sample in **Figure 8a**. The cooling cycle shows a more pronounced heat retention effect, with temperatures decreasing at a slower rate in **Figure 8d**. These results highlight the effectiveness of PCM in moderating temperature fluctuations in concrete pavements. Additionally, the increasing gap between the top and bottom curves during the heating phase, as shown in **Figure 8**, indicates the effective heat absorption and storage capabilities of PCM. For the 0% PCM sample the gap is the smallest, representing a direct temperature rise due to applied heat. In contrast, the 5% PCM sample and the 10% PCM sample show progressively larger gaps. This illustrates that higher PCM content enhances thermal regulation by delaying and moderating the surface temperature rise, leading to a more pronounced differential between the bottom and the top temperatures.

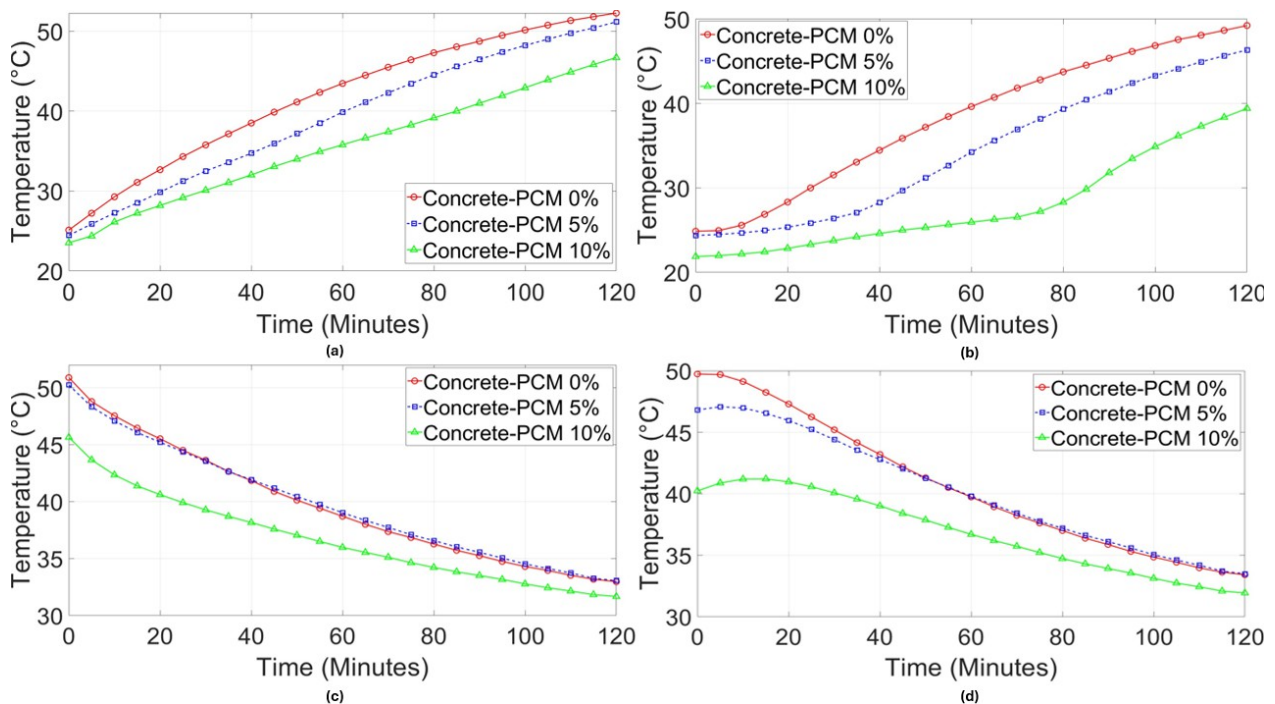


Figure 8: Heating cycle for two hours: (a) Top Surface; (b) Bottom Surface. Cooling Cycle for two hours: (c) Top Surface; (d) Bottom Surface.

Indoor Results -Pavement surface temperature observations by Sand-Replacement Method

Figure 9 presents the surface temperature profiles for concrete samples containing 0%, 5%, and 10% R-PCM, integrated through Sand-Replacement Method, observed over a four-hour period. During the heating cycle, the 0% R-PCM sample in **Figure 9a** displayed the highest temperature increase, with both the top and bottom surfaces reaching their peak temperatures faster than the samples containing PCM. The top surface in particular exhibited a more pronounced temperature rise, mirroring the trend seen in the bottom surface. As anticipated, the cooling cycle in **Figure 9c** for the 0% R-PCM sample showed a consistent temperature decrease across both surfaces, with minimal variation between the top and bottom, indicating a uniform heat dissipation without the influence of PCM. In contrast, the 5% R-PCM sample in **Figure 9a** showed a slower rate of temperature increase during the heating cycle. Although the top surface still heated up faster than the bottom, the maximum temperatures reached were approximately 2°C lower than those observed in the 0% R-PCM sample. During the cooling phase, the temperature decline in the 5% R-PCM sample was more gradual. However, as the cooling progressed, the temperature curve of the 5% R-PCM sample began to converge with that of the 0% R-PCM sample, suggesting a diminishing differential as the cooling cycle continued. The 10% R-PCM sample in **Figure 9a** exhibited the most substantial temperature reduction during the heating cycle, with peak temperatures for both surfaces being around 3°C lower than those of the 0% R-PCM sample. In the cooling cycle in **Figure 9d**, the temperature decreases for the 10% R-PCM sample showed no significant difference between the top and bottom surfaces, maintaining a consistent reduction throughout the period.

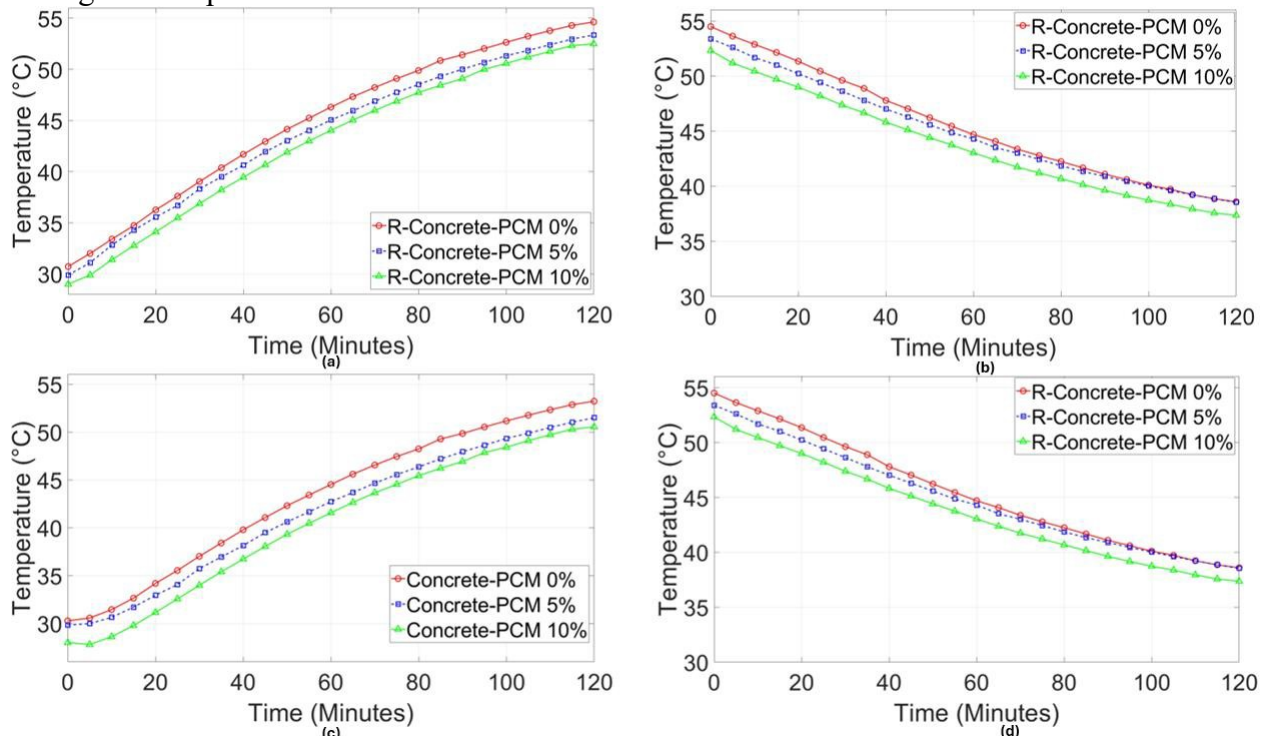


Figure 9: Heating cycle for two hours: (a) Top Surface; (b) Bottom Surface. Cooling Cycle for two hours: (c) Top Surface; (d) Bottom Surface

Materials testing Results

Figure 10 presents the thermal properties of concrete samples with 0%, 5%, and 10% PCM integrated through the Addition Method, showcasing the apparent specific heat capacity, thermal

conductivity, and thermal diffusivity across a range of temperatures from 25°C to 80°C. As shown in **Figure 10a**, the apparent specific heat capacity (C_p) of the concrete samples varies with temperature. The 5% and 10% PCM samples exhibit a significant increase in specific heat capacity as the temperature approaches the PCM melting point, around 30°C to 35°C. The 5% PCM sample shows a noticeable rise in specific heat capacity at this temperature, reflecting the latent heat absorption during the phase change of the PCM. The 10% PCM sample demonstrates an even larger increase, indicating a greater capacity to store heat due to the higher PCM content. After surpassing the PCM melting point, the specific heat capacity of both PCM-enhanced samples decreases and stabilizes, aligning more closely with the 0% PCM sample as the temperature continues to rise. To accurately reflect the nature of the heat capacity observed, the label of the y-axis in **Figure 10a** is named as “apparent specific heat.” This term encompasses both sensible and latent heat components, explaining the elevated values in the 20-35°C range for PCM-containing materials. **Figure 10b** illustrates the thermal conductivity of the concrete samples. The 0% PCM sample maintains a high and relatively stable thermal conductivity throughout the temperature range, which is characteristic of standard concrete’s efficient heat conduction properties. The 5% and 10% PCM samples, however, show a distinct reduction in thermal conductivity, particularly near the PCM melting point. The 5% PCM sample experiences a moderate decrease in thermal conductivity, while the 10% PCM sample shows a more substantial reduction. This decrease is indicative of the PCM's phase change, which disrupts the heat transfer pathways within the concrete, effectively lowering its ability to conduct heat. Thermal diffusivity, depicted in **Figure 10c**, measures how quickly heat spreads through the material. The 0% PCM sample exhibits relatively high thermal diffusivity, indicating its ability to rapidly absorb and distribute heat. The 5% PCM sample shows a reduction in thermal diffusivity near the PCM melting point, consistent with the observed decrease in thermal conductivity. The 10% PCM sample shows an even further reduction in thermal diffusivity, suggesting that the PCM not only absorbs more heat but also slows the rate at which this heat spreads through the material. This lower thermal diffusivity indicates enhanced thermal buffering, as the PCM slows the material's response to temperature changes.

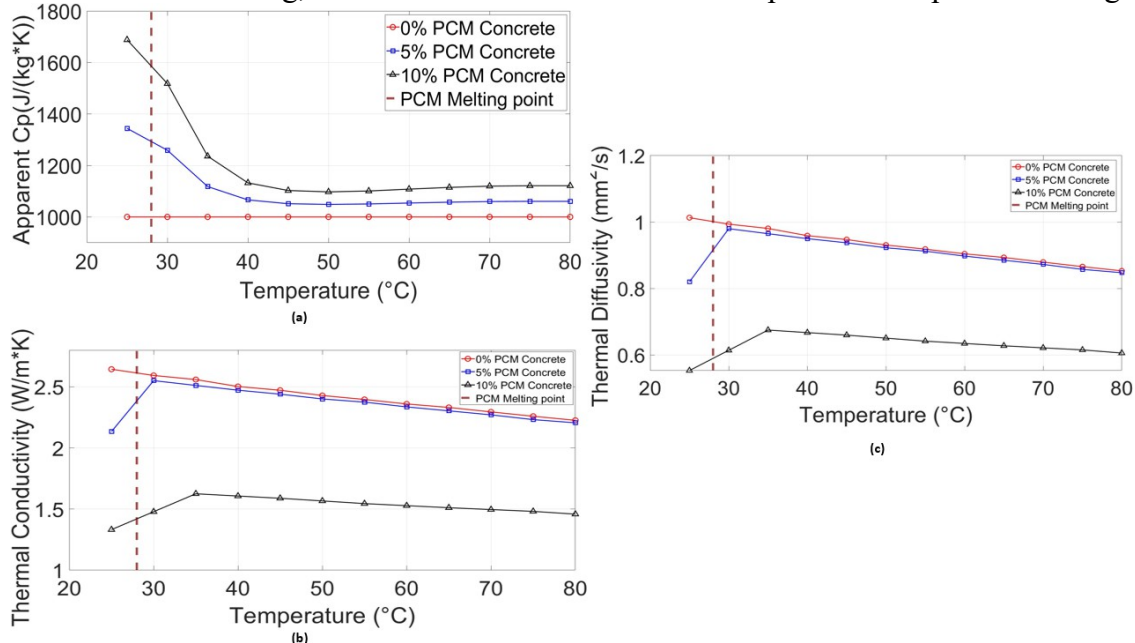


Figure 10: Thermal Properties comparison of Addition Method; (a) Apparent Specific Heat Capacity; (b) Thermal Conductivity; (c) Thermal Diffusivity.

Figure 11 presents the thermal properties of concrete samples with 0%, 5%, and 10% R-PCM integrated through the Sand-Replacement Method, showcasing the apparent specific heat capacity, thermal conductivity, and thermal diffusivity across a range of temperatures from 25°C to 80°C. As depicted in **Figure 11a**, the apparent specific heat capacity (C_p) of the concrete samples shows distinct variations with temperature, particularly around the PCM melting point at 30°C to 35°C. The 5% and 10% R-PCM samples exhibit a marked increase in specific heat capacity as the temperature approaches the PCM melting point. The 5% R-PCM sample shows a noticeable rise in specific heat capacity in this temperature range, indicating the absorption of latent heat as the PCM undergoes its phase transition. The 10% R-PCM sample demonstrates an even more significant increase, reflecting the higher PCM content's ability to store more heat. After the PCM completes its phase transition, the specific heat capacity of both PCM-enhanced samples decreases and stabilizes, aligning more closely with the 0% R-PCM sample at higher temperatures. **Figure 11b** illustrates the thermal conductivity of the concrete samples. The 0% R-PCM sample exhibits high and stable thermal conductivity throughout the temperature range, consistent with the heat conduction properties expected of standard concrete. The integration of PCM via sand-replacement, however, leads to a noticeable reduction in thermal conductivity, especially around the PCM melting point. The 5% R-PCM sample experiences a moderate decrease in thermal conductivity, while the 10% R-PCM sample shows a more substantial reduction. This reduction is indicative of the PCM's phase change, which disrupts the continuity of heat conduction pathways within the concrete matrix, thereby lowering the material's overall ability to conduct heat. The 0% R-PCM sample has relatively high thermal diffusivity in **Figure 11c**, indicating its ability to rapidly absorb and distribute heat throughout the concrete. The 5% R-PCM sample shows a reduction in thermal diffusivity near the PCM melting point, consistent with the observed decrease in thermal conductivity. The 10% R-PCM sample exhibits an even further reduction in thermal diffusivity, suggesting that the increased PCM content not only enhances the material's heat storage capacity but also slows the rate at which heat is transferred within the concrete.

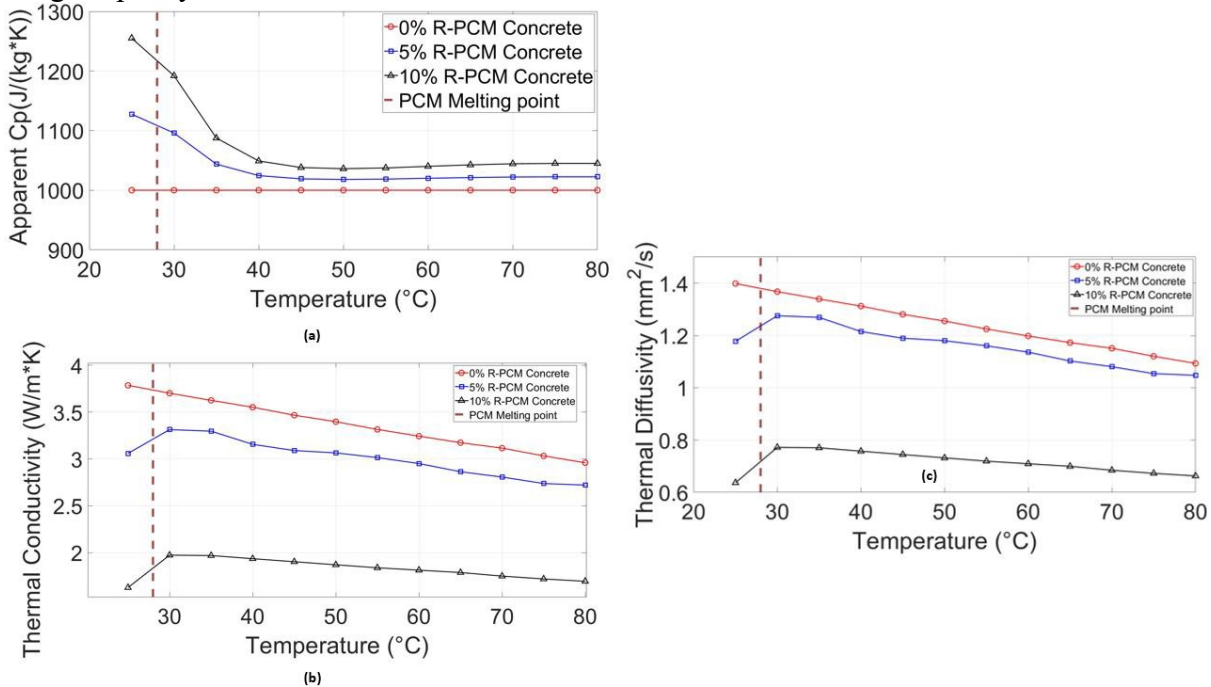


Figure 11: Thermal Properties comparison of Sand-Replacement Method; (a) Apparent Specific Heat Capacity; (b) Thermal Conductivity; (c) Thermal Diffusivity.

Pavement System Design

Focusing on developing a concrete pavement capable of regulating temperature through the integration of PCM. This process began with assessing the thermal properties of the chosen PCM, including melting point and heat of fusion, to ensure compatibility with pavement applications. Multiple PCM dosages were then tested within the concrete mix, and their effects on key thermal properties—such as thermal conductivity, diffusivity, and specific heat capacity. The collected data guided the refinement of PCM dosage levels, balancing thermal performance with the structural integrity required for a durable, high-performing pavement system. The design is now optimized to deliver both effective temperature control and long-term resilience in UHI mitigation.

Field Implementation and Monitoring

The field implementation and monitoring phase has been successfully completed, focusing on the real-world performance of PCM-enhanced concrete in mitigating temperature fluctuations in pavement applications. These outdoor experiments were designed to simulate natural environmental conditions, with the concrete slabs exposed to peak sunlight from 1 to 9 pm, for a total of 8 hours. The samples, placed in direct sunlight, were equipped with temperature sensors to track the behavior of PCM in response to heat during the day as shown in **Figure 12**. The data collected allowed us to evaluate how effectively PCM reduced surface temperatures as shown in **Figure 13**. In addition to daytime heating, the nighttime cooling phase was also crucial. As temperatures dropped, the experiment assessed how the stored heat in PCM was released, providing insights into its ability to slow the cooling rate. This overnight cooling period helped in understanding how PCM can reduce temperature-related stresses in the pavement, enhancing its overall durability and resilience under real-world conditions.



Figure 12: Outdoor experiments, (a) During day, (b) During night.

Outdoor Results

Figure 13 illustrates the surface temperature profiles for concrete samples with 0%, 5%, and 10% PCM, integrated through both the addition and sand-replacement methods, over an 8-hour outdoor exposure cycle. This cycle includes natural heating from solar radiation followed by cooling as the ambient temperature drops. In the addition method, as shown in **Figure 13a** (top surface) and **Figure 13b** (bottom surface), the 0% PCM sample exhibited the highest peak temperatures, particularly on the top surface, which reached approximately 47°C. This behavior is typical of unmodified concrete, which rapidly absorbs and conducts heat, leading to significant temperature increases under direct sunlight. The 5% PCM sample displayed a moderate reduction in peak temperature within the midday peak, with the top surface temperature reduced by approximately 2°C compared to the 0% PCM sample in **Figure 13a**. Then, it was slightly higher than the 0% PCM sample during releasing the heat when the surrounding temperature started to drop. The

bottom surface showed a similar reduction, indicating that PCM was effective in moderating heat absorption during the peak exposure period. The 10% PCM sample demonstrated the most significant temperature reduction, with a peak temperature of around 40°C on the top surface, representing a 7°C decrease compared to the 0% PCM sample in **Figure 13a**. The bottom surface exhibited a similar pattern, with temperatures consistently lower than those of the 5% PCM and 0% PCM samples in **Figure 13b**. The results for the Sand-Replacement Method, depicted in **Figure 13c** (top surface) and **Figure 13d** (bottom surface), present a different thermal behavior profile. The 0% R-PCM sample again exhibited the highest peak temperatures, with the top surface reaching around 50°C. The 5% R-PCM sample in the sand-replacement method showed a small reduction in peak temperature, with the top surface temperature approximately 1.5°C lower than that of the 0% R-PCM sample in **Figure 13c**. This reduction is more modest than the reduction observed in the addition method, suggesting that the lower PCM content in the sand-replacement method has a limited impact on temperature moderation. The 10% R-PCM sample in the sand-replacement method exhibited a peak temperature of around 46°C on the top surface, indicating a 4°C reduction compared to the 0% R-PCM sample in **Figure 13c**. While this reduction is significant, it is less pronounced than the 7°C reduction observed in the Addition Method, highlighting the limitations of the Sand-Replacement Method in achieving substantial thermal regulation.

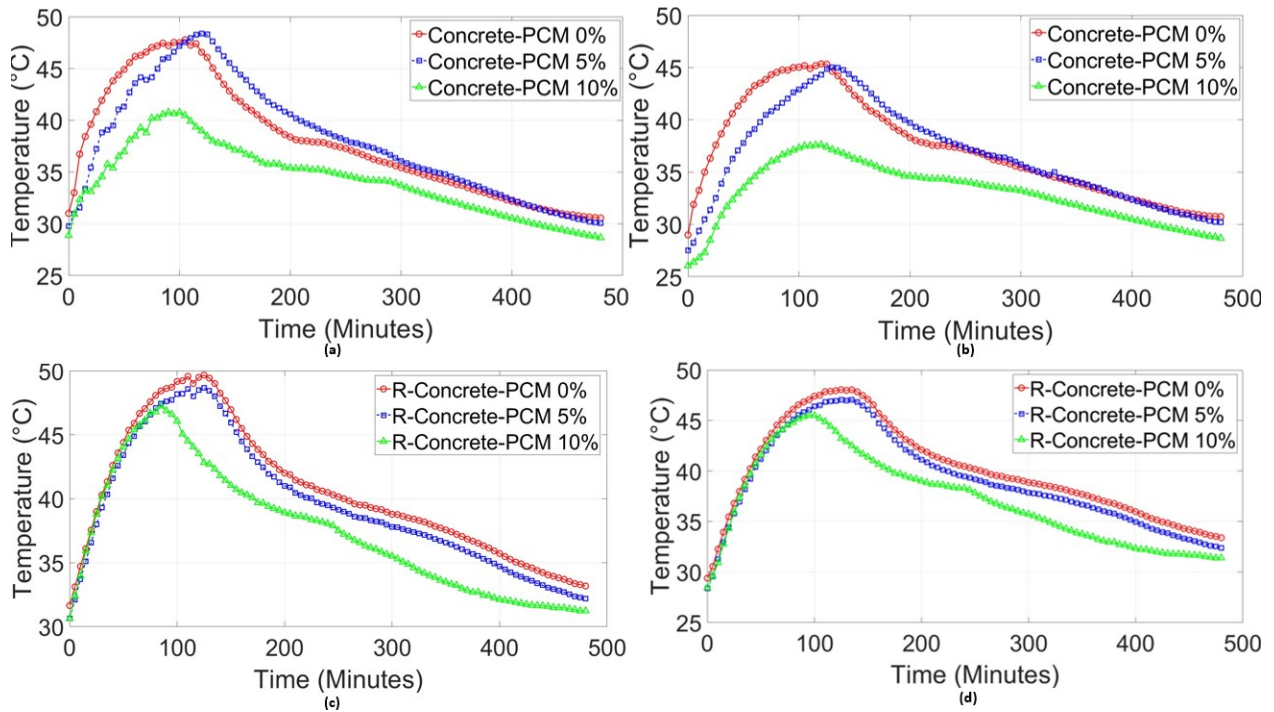


Figure 13: Outdoor exposure cycle for 8 hours. Addition: (a) Top Surface; (b) Bottom Surface. Sand-Replacement: (c) Top Surface; (d) Bottom Surface

Educational outreach and workforce development

- Summary of the project was presented to undergraduates in the CE 3243 class. *Feb 2024*.
- A summary of the project was presented to the Highway Engineering CE 3223, *Feb 2024*.
- Demo and tour to UTSA prospective students, emphasizing urban challenges, *July 2024*.

- Promoting Trans-IPIC center in an outreach event at Champion High School, Boerne, TX *November 2024* (Figure 14)



Figure 14: Educational Outreach Events

Technology Transfer

- **Microtek Laboratories, Inc.:** Shared our experimental results, highlighting the temperature reduction achieved in precast concrete integrated with PCM. These results provide insight into the thermal performance improvements enabled by PCM.
- **Tindall Corporation:** Collaborated in several meetings to share our design mix details for scaling up the project. Leveraged Tindall's expertise in precast concrete to refine and adapt the design for large-scale implementation.

Papers that include TRANS-IPIC UTC in the acknowledgments section

- Accepted manuscript for presentation at the TRB Annual Meeting, *Jan 2025*.
- Prepared manuscript for submission to Int. J. of Pavement Engineering, *Dec 2024*
- Prepared manuscript for submission to J. of Construction and Building Materials, *Dec 2024*. (*under review*)

Number of presentations

- Presented in the Highways USA conference, *October 2023*.
 - ❖ Radwan, I. and Dessouky, S. “Cool Pavements for Mitigating UHI Effect using PCM in Precast Concrete.” Highways USA Conference, October 2023.
- Presented in the TRANS-IPIC Monthly Research Webinar, *March 2024*.
 - ❖ Radwan, I. and Dessouky, S. “Cool Pavements for Mitigating UHI Effect using PCM in Precast Concrete” *Transportation Infrastructure Precast Innovation Center (TRANS-IPIC) Monthly Research Webinar*. March 4th. 2024.
- Presented in the TRANS-IPIC Workshop and engaged with industry experts, *April 2024*
 - ❖ Radwan, I. and Dessouky, S. “Cool Pavements for Mitigating UHI Effect using PCM in Precast Concrete” *Transportation Infrastructure Precast Innovation Center (TRANS-IPIC) Workshop, Presentation*. April 22nd. 2024.
- Presented poster in the USDOT Future of Transportation Summit, *August 2024*.
 - ❖ Radwan, I. and Dessouky, S. “Cool Pavements for Mitigating UHI Effect using PCM in Precast Concrete.” USDOT Future of Transportation Summit, August 2024
- Presented in the UTSA Klesse Research Expo, *November 2024*.
 - ❖ Radwan, I. and Dessouky, S. “Cool Pavements for Mitigating UHI Effect using PCM in Precast Concrete.” UTSA Klesse Research Expo, November 18th, 2024.



Figure 15: Research presentations in conferences and events

REFERENCES

- [1] T. R. Oke, “The energetic basis of the urban heat island,” *Quart J Royal Meteorol Soc*, vol. 108, no. 455, pp. 1–24, Jan. 1982, doi: 10.1002/qj.49710845502.
- [2] Oke, T. R. (1988). *The urban energy balance*. *Progress in Physical Geography*, 12(4), 471–508. <https://doi.org/10.1177/030913338801200401>
- [3] A. J. Arnfield, “Two decades of urban climate research: a review of turbulence, exchanges of energy and water, and the urban heat island,” *Int. J. Climatol.*, vol. 23, no. 1, pp. 1–26, Jan. 2003, doi: 10.1002/joc.859.
- [4] K. S. Al-Jabri, A. W. Hago, A. S. Al-Nuaimi, and A. H. Al-Saidy, “Concrete blocks for thermal insulation in hot climate,” *Cement and Concrete Research*, vol. 35, no. 8, pp. 1472–1479, Aug. 2005, doi: 10.1016/j.cemconres.2004.08.018.
- [5] C. S. B. Grimmond and T. R. Oke, “Heat Storage in Urban Areas: Local-Scale Observations and Evaluation of a Simple Model,” *J. Appl. Meteor.*, vol. 38, no. 7, pp. 922–940, Jul. 1999, doi: 10.1175/1520-0450(1999)038<0922:HSIUAL>2.0.CO;2.
- [6] K. Fortuniak, “Numerical estimation of the effective albedo of an urban canyon,” *Theor Appl Climatol*, vol. 91, no. 1–4, pp. 245–258, Feb. 2008, doi: 10.1007/s00704-007-0312-6.
- [7] Y. Qin and J. E. Hiller, “Understanding pavement-surface energy balance and its implications on cool pavement development,” *Energy and Buildings*, vol. 85, pp. 389–399, Dec. 2014, doi: 10.1016/j.enbuild.2014.09.076.
- [8] K. Anandakumar, “A study on the partition of net radiation into heat fluxes on a dry asphalt surface,” *Atmospheric Environment*, 1999.
- [9] H. Akbari and L. S. Rose, “Characterizing the fabric of the urban environment: A case study of Metropolitan Chicago, Illinois and Executive Summary,” LBNL--49275, Oct. 2001. doi: 10.2172/900694.

- [10] H. Akbari, L. S. Rose, and H. Taha, “Characterizing the Fabric of the Urban Environment: A Case Study of Sacramento, California,” LBNL-44688, 764362, Dec. 1999. doi: 10.2172/764362.
- [11] H. Li, “Evaluation of Cool Pavement Strategies for Heat Island Mitigation”.
- [12] H. Akbari, M. Pomerantz, and H. Taha, “Cool surfaces and shade trees to reduce energy use and improve air quality in urban areas,” *Solar Energy*, vol. 70, no. 3, pp. 295–310, 2001, doi: 10.1016/S0038-092X(00)00089-X.
- [13] L. Gartland, *Heat islands: understanding and mitigating heat in urban areas*. London; Sterling, VA: Earthscan, 2008.
- [14] H. Akbari, “Energy Saving Potentials and Air Quality Benefits of Urban Heat Island Mitigation”.
- [15] Y. Yamashita, K. Sakamoto, H. Akiyoshi, M. Takahashi, T. Nagashima, and L. B. Zhou, “Ozone and temperature response of a chemistry climate model to the solar cycle and sea surface temperature,” *J. Geophys. Res.*, vol. 115, no. D3, p. 2009JD013436, Feb. 2010, doi: 10.1029/2009JD013436.
- [16] B. J. Bloomer, J. W. Stehr, C. A. Piety, R. J. Salawitch, and R. R. Dickerson, “Observed relationships of ozone air pollution with temperature and emissions,” *Geophysical Research Letters*, vol. 36, no. 9, p. 2009GL037308, May 2009, doi: 10.1029/2009GL037308.
- [17] M. Pomerantz, H. Akbari, L. B. Laboratory, and J. T. Harvey, “Cooler Reflective Pavements Give Benefits Beyond Energy Savings: Durability and Illumination”.
- [18] Young, M., et al., “‘Field application of PCM in concrete pavement,’ *Energy and Buildings*, 2016, 122: 228-234.”.
- [19] Wei, H., et al., “‘Phase change materials for thermal regulation of concrete,’ *Journal of Cleaner Production*, 2017, 162: 1182-1191.”.
- [20] Lin, K.P., et al., “‘Experimental study on microencapsulated PCM for thermal management,’ *Energy Conversion and Management*, 2005, 46(6): 847-861.”.
- [21] Y. Farnam, H. S. Esmaeeli, P. D. Zavattieri, J. Haddock, and J. Weiss, “Incorporating phase change materials in concrete pavement to melt snow and ice,” *Cement and Concrete Composites*, vol. 84, pp. 134–145, Nov. 2017, doi: 10.1016/j.cemconcomp.2017.09.002.
- [22] D. P. Bentz and R. Turpin, “Potential applications of phase change materials in concrete technology,” *Cement and Concrete Composites*, vol. 29, no. 7, pp. 527–532, Aug. 2007, doi: 10.1016/j.cemconcomp.2007.04.007.
- [23] Y. Farnam, A. Wiese, D. Bentz, J. Davis, and J. Weiss, “Damage development in cementitious materials exposed to magnesium chloride deicing salt,” *Construction and Building Materials*, vol. 93, pp. 384–392, Sep. 2015, doi: 10.1016/j.conbuildmat.2015.06.004.
- [24] M. Hunger, A. G. Entrop, I. Mandilaras, H. J. H. Brouwers, and M. Founti, “The behavior of self-compacting concrete containing micro-encapsulated Phase Change Materials,” *Cement and Concrete Composites*, vol. 31, no. 10, pp. 731–743, Nov. 2009, doi: 10.1016/j.cemconcomp.2009.08.002.
- [25] Ramakrishnan, S., et al., “Influence of phase change material (PCM) on the properties of concrete. *Cement and Concrete Research*, 96, 26-35” 2017.
- [26] Jayalath, A., et al., “Thermal properties of concrete with microencapsulated phase change materials. *Journal of Materials in Civil Engineering*, 28(7), 04016034,” 2016.